

Synthesis, Electrochemistry, Photophysics, and Solvatochromism in New Cyclometalated 6-Phenyl-4-(*p*-R-phenyl)-2,2'-bipyridyl (R = Me, COOMe, P(O)(OEt)₂) (C[^]N[^]N) Platinum(II) Thiophenolate Chromophores

Jacob Schneider, Pingwu Du, Xiaoyong Wang, William W. Brennessel, and Richard Eisenberg*

Department of Chemistry, University of Rochester, Rochester, New York 14627

Received September 15, 2008

Three new cyclometalated 6-phenyl-4-(*p*-R-phenyl)-2,2'-bipyridyl (C[^]N[^]N) Pt(II) thiophenolate complexes (R = Me (**2a**), COOMe (**2b**), and P(O)(OEt)₂ (**2c**)) have been synthesized and studied. The new C[^]N[^]N ligands **L2** (R = COOMe) and **L3** (R = P(O)(OEt)₂) undergo cyclometalation with a Pt(II) source to give the Pt(II) chloro complexes **1b** and **1c**, respectively, which are luminescent in fluid solution with $\lambda_{\text{max}} \sim 575$ nm, assigned to a metal-to-ligand charge-transfer (³MLCT) emissive state. Reaction of the chloro complexes **1a** (R = Me), **1b**, and **1c** with sodium thiophenolate gives **2a–2c**, respectively, in good yields. The novel thiophenolate complexes have two interesting absorption bands in their electronic spectra tentatively assigned to a charge-transfer to C[^]N[^]N (¹CT) ($\lambda_{\text{abs}} \sim 415$ nm) transition and a mixed metal/ligand-to-ligand' charge-transfer (MMLL'CT, $\lambda_{\text{abs}} \sim 555$ nm) transition, respectively. The MMLL'CT band is solvatochromic with absorption maxima in the range of 496 nm in MeOH to 590 nm in toluene ($\epsilon \sim 4000$ dm³ mol⁻¹ cm⁻¹), which correlate well with an empirical charge-transfer-based solvent scale. Excitation of **2a–2c** into the MMLL'CT band gives emission maxima around 680 nm in frozen CH₂Cl₂ solution, and no emission in fluid solution. Ligand **L2** and complexes **1a**·MeCN, **1b**, and **2b**·CH₂Cl₂ have been characterized by single crystal X-ray crystallography. The electrochemical properties of ligands **L1** (R = Me) and **L2** and complexes **1a–1c** and **2a–2c** have been examined by cyclic voltammetry and are shown to exhibit reversible and quasi-reversible reductions and irreversible oxidations.

Introduction

Square planar platinum(II) complexes are known to have a rich history of photochemical and photophysical properties,¹ due in part to their high quantum efficiencies and the nature of their excited states.^{2–4} One set of these complexes consists of platinum(II) bi- and terpyridyl systems that have recently received attention for possible use in a range of applications including biosensing,^{5–7} intercalation into

DNA,^{8–10} electroluminescent materials in light-emitting devices (LEDs),^{11,12} chromophores for photoinduced charge separation and energy storage,^{13–16} and sensitizers in the

* To whom correspondence should be addressed. E-mail: eisenberg@chem.rochester.edu.

- (1) Williams, J. A. G. *Top. Curr. Chem.* **2007**, *281*, 205–268.
- (2) Shikhova, E.; Danilov, E. O.; Kinayyigit, S.; Pomestchenko, I. E.; Tregubov, A. D.; Camerel, F.; Retailleau, P.; Ziessel, R.; Castellano, F. N. *Inorg. Chem.* **2007**, *46*, 3038–3048.
- (3) Yang, Q.-Z.; Wu, L.-Z.; Wu, Z.-X.; Zhang, L.-P.; Tung, C.-H. *Inorg. Chem.* **2002**, *41*, 5653–5655.
- (4) Weinstein, J. A.; Grills, D. C.; Towrie, M.; Matousek, P.; Parker, A. W.; George, M. W. *Chem. Commun.* **2002**, 382–383.
- (5) Lo, H.-S.; Yip, S.-K.; Wong, K. M.-C.; Zhu, N.; Yam, V. W.-W. *Organometallics* **2006**, *25*, 3537–3540.
- (6) Wong, K. M.-C.; Tang, W.-S.; Lu, X.-X.; Zhu, N.; Yam, V. W.-W. *Inorg. Chem.* **2005**, *44*, 1492–1498.

- (7) Yu, C.; Chan, K. H.-Y.; Wong, K. M.-C.; Yam, V. W.-W. *Proc. Natl. Acad. Sci. U.S.A.* **2006**, *103*, 19652–19657.
- (8) Brodie, C. R.; Collins, J. G.; Aldrich-Wright, J. R. *Dalton Trans.* **2004**, 1145–1152.
- (9) Wheate, N. J.; Taleb, R. I.; Krause-Heuer, A. M.; Cook, R. L.; Wang, S.; Higgins, V. J.; Aldrich-Wright, J. R. *Dalton Trans.* **2007**, 5055–5064.
- (10) Lu, W.; Vicic, D. A.; Barton, J. K. *Inorg. Chem.* **2005**, *44*, 7970–7980.
- (11) Chang, S.-Y.; Kavitha, J.; Hung, J.-Y.; Chi, Y.; Cheng, Y.-M.; Li, E. Y.; Chou, P.-T.; Lee, G.-H.; Carty, A. J. *Inorg. Chem.* **2007**, *46*, 7064–7074.
- (12) Liu, Q.; Thorne, L.; Kozin, I.; Song, D.; Seward, C.; D'Iorio, M.; Tao, Y.; Wang, S. *J. Chem. Soc., Dalton Trans.* **2002**, 3234–3240.
- (13) Chakraborty, S.; Wadas, T. J.; Hester, H.; Flaschenreim, C.; Schmehl, R.; Eisenberg, R. *Inorg. Chem.* **2005**, *44*, 6284–6293.
- (14) Chakraborty, S.; Wadas, T. J.; Hester, H.; Schmehl, R.; Eisenberg, R. *Inorg. Chem.* **2005**, *44*, 6865–6878.
- (15) McGarrah, J. E.; Eisenberg, R. *Inorg. Chem.* **2003**, *42*, 4355–4365.
- (16) Wadas, T. J.; Chakraborty, S.; Lachicotte, R. J.; Wang, Q.-M.; Eisenberg, R. *Inorg. Chem.* **2005**, *44*, 2628–2638.

photocatalytic generation of hydrogen from water.^{17–19} Interestingly, many of these di- and triimine square-planar complexes exhibit solvatochromism in which the energies and intensities of charge-transfer excited state transitions are influenced by solvent polarity.²⁰ For Pt(diimine)(dithiolate) complexes, the solvatochromic absorption band is a low energy transition corresponding to an excited state that involves a highest occupied molecular orbital (HOMO) of both metal and dithiolate character and a lowest unoccupied molecular orbital (LUMO) that is a π^* function of the diimine ligand.^{21,22} More recent studies on bis(phenolate) and bis(thiolate) Pt(II) diimine complexes exhibit similar behavior with likewise HOMO assignments of mixed Pt/O or Pt/S character.²³ In a study of the terpyridyl complex, [Pt(tpy)(C \equiv C–C \equiv CH)]⁺ (tpy = 2,2'–6',2''-terpyridine), Yam and co-workers attributed the appreciable color change and emission enhancement in different solvent mixtures to a solvatochromic effect modified by metal-metal and π - π stacking interactions.²⁴

A separate set of Pt(II) cyclometalated complexes that include C \wedge N, C \wedge N \wedge N,^{25–27} C \wedge N \wedge C,^{28–30} C \wedge N \wedge C,^{31–34} and N \wedge C \wedge N derivatives^{35,36} are analogous to the aforementioned bi- and terpyridyl complexes and possess desirable photophysical properties as well.³⁷ In fact cyclometalated Pt(II)(C \wedge N \wedge N) complexes have been of interest for many of the same applications, including luminescent molecular sensors,³⁸ metallointercalators,³⁹ and dopant emitters in LEDs.^{40,41}

In this article, we report three novel cyclometalated Pt(C \wedge N \wedge N) thiophenolate complexes (**2a–2c**) having a

solvatochromic lowest energy absorption band. The synthesis of two new 6-phenyl-4-(*p*-R-phenyl)-2,2'-bipyridyl C \wedge N \wedge N ligands is described for R = COOMe (**L2**) and P(O)(OEt)₂ (**L3**), and cyclometalation of these ligands to a Pt(II) chloride source yields neutral luminescent Pt(C \wedge N \wedge N)Cl complexes. Treatment of these chloride complexes with sodium thiophenolate gives dark purple solids that possess lowest energy absorption maxima assignable to mixed metal/ligand-to-ligand' charge-transfer (MMLL'CT) transitions. The new complexes are characterized electrochemically and spectroscopically and in several cases crystallographically.

Experimental Section

Characterization and Instrumentation. All NMR spectra were recorded using either Bruker Avance 400 or 500 MHz spectrometers. ¹H NMR chemical shifts (in ppm) are referenced using the chemical shift of CDCl₃ or DMSO-*d*₆. ³¹P NMR chemical shifts (in ppm) are relative to an external 85% solution of H₃PO₄ in the appropriate solvent. Mass determinations were accomplished by atmospheric pressure chemical ionization (APCI) mass spectrometry using a Hewlett-Packard Series 1100 mass spectrometer (model A) equipped with a quadrupole mass filter. Elemental analyses were performed by Quantitative Technologies Inc. (QTI). Absorption spectra were recorded using a Hitachi U2000 scanning spectrophotometer (200–1100 nm). Steady-state emission spectra were obtained using a Spex Fluoromax-P fluorimeter corrected for instrument response with monochromators positioned with a 2 nm band-pass. The metal complex concentration of solution samples was 1.0 \times 10^{–5} M in CH₂Cl₂ for complexes **1a–1c** and 2.1 \times 10^{–5} M in CH₂Cl₂ for complexes **2a–2c**. Each sample was degassed by at least two freeze–pump–thaw cycles. The room temperature emission quantum yields (ϕ_{em}) are measured relative to Ru(bpy)₃Cl₂ in degassed H₂O as the reference solution (ϕ_{em} = 0.042).⁴² They were calculated using eq 1

$$\phi_s = \phi_r(I_s/I_r)(A_r/A_s)(n_s^2/n_r^2) \quad (1)$$

where the subscripts s and r, respectively, denote sample and reference; *I* is the integrated emission intensity; *A* is the absorbance in a dilute solution ($\sim 10^{-5}$ M, *A* < 0.5) at the wavelength of excitation; and *n* is the refractive index that corrects for differences between the reference and the sample solutions.⁴³

Excited state lifetime measurements of deoxygenated CH₂Cl₂ solution samples ($\sim 10^{-4}$ M) of complexes **1a–1c** and **2a–2c** were obtained by frequency doubling and pulse picking a femtosecond Ti-Sapphire laser at 450 nm (complexes **1a–1c**) and 403 nm (complexes **2a–2c**) with a 3.8 MHz repetition rate. The laser beam was focused on the samples in a quartz cuvette by a microscope objective (50 \times , NA 0.55) with a power density of ~ 1 kW/cm^{–1}. The photoluminescence (PL) from the samples was collected by the same objective and sent through a 0.5 m spectrometer to a charge coupled device (CCD) camera or a time-correlated single

- (17) Du, P.; Schneider, J.; Jarosz, P.; Eisenberg, R. *J. Am. Chem. Soc.* **2006**, *128*, 7726–7727.
- (18) Du, P.; Schneider, J.; Jarosz, P.; Zhang, J.; Brennessel, W. W.; Eisenberg, R. *J. Phys. Chem. B* **2007**, *111*, 6887–6894.
- (19) Zhang, J.; Du, P.; Schneider, J.; Jarosz, P.; Eisenberg, R. *J. Am. Chem. Soc.* **2007**, *129*, 7726–7727.
- (20) Hirayama, S.; Steer, R. P. *J. Chem. Educ.* **2008**, *85*, 317–319.
- (21) Cummings, S. D.; Eisenberg, R. *J. Am. Chem. Soc.* **1996**, *118*, 1949–1960.
- (22) Cummings, S. D.; Eisenberg, R. *Inorg. Chem.* **1995**, *34*, 2007–2014.
- (23) Weinstein, J. A.; Tierney, M. T.; Davies, E. S.; Base, K.; Roberio, A. A.; Grinstaff, M. W. *Inorg. Chem.* **2006**, *45*, 4544–4555.
- (24) Yam, V. W.-W.; Wong, K. M.-C.; Zhu, N. *J. Am. Chem. Soc.* **2002**, *124*, 6506–6507.
- (25) Hirani, B.; Li, J.; Djurovich, P. I.; Yousufuddin, M.; Oxgaard, J.; Persson, P.; Wilson, S. R.; Bau, R.; Goddard, W. A., III; Thompson, M. E. *Inorg. Chem.* **2007**, *46*, 3865–3875.
- (26) Furuta, P. T.; Deng, L.; Garon, S.; Thompson, M. E.; Frechet, J. M. J. *J. Am. Chem. Soc.* **2004**, *126*, 15388–15389.
- (27) Minghetti, G.; Stoccoro, S.; Cinellu, M. A.; Soro, B.; Zucca, A. *Organometallics* **2003**, *22*, 4770–4777.
- (28) Lu, W.; Mi, B.-X.; Chan, M. C. W.; Hui, Z.; Che, C.-M.; Zhu, N.; Lee, S.-T. *J. Am. Chem. Soc.* **2004**, *126*, 4958–4971.
- (29) Lai, S.-W.; Chan, M. C.-W.; Cheung, T.-C.; Peng, S.-M.; Che, C.-M. *Inorg. Chem.* **1999**, *38*, 4046–4055.
- (30) Lai, S. W.; Chan, M. C.-W.; Cheung, K.-K.; Che, C.-M. *Organometallics* **1999**, *18*, 3327–3336.
- (31) Cave, G. W. V.; Fanizzi, F. P.; Deeth, R. J.; Errington, W.; Rourke, J. P. *Organometallics* **2000**, *19*, 1355–1364.
- (32) Lu, W.; Chan, M. C. W.; Cheung, K.-K.; Che, C.-M. *Organometallics* **2001**, *20*, 2477–2486.
- (33) Kui, S. C. F.; Chui, S. S.-Y.; Che, C.-M.; Zhu, N. *J. Am. Chem. Soc.* **2006**, *128*, 8297–8309.
- (34) Berenguer, J. R.; Lalinde, E.; Torroba, J. *Inorg. Chem.* **2007**, *46*, 9919–9930.
- (35) Williams, J. A. G.; Beeby, A.; Davies, E. S.; Weinstein, J. A.; Wilson, C. *Inorg. Chem.* **2003**, *42*, 8609–8611.
- (36) Sotoyama, W.; Satoh, T.; Sawatari, N.; Inoue, H. *Appl. Phys. Lett.* **2005**, *86*, 153505.
- (37) Lai, S.-W.; Che, C.-M. *Top. Curr. Chem.* **2004**, *241*, 27–63.

- (38) Yang, Q.-Z.; Wu, L.-Z.; Zhang, H.; Chen, B.; Wu, Z.-X.; Zhang, L.-P.; Tung, C.-H. *Inorg. Chem.* **2004**, *43*, 5195–5197.
- (39) Che, C.-M.; Zhang, J.-L.; Lin, L.-R. *Chem. Commun.* **2002**, 2556–2557.
- (40) Lu, W.; Mi, B.-X.; Chan, M. C. W.; Hui, Z.; Zhu, N.; Lee, S.-T.; Che, C.-M. *Chem. Commun.* **2002**, 206–207.
- (41) Che, C.-M.; Lu, W.; Chan, M. C.-W. Application: U.S.; The University of Hong Kong: Hong Kong 2002; p 21.
- (42) Van Houten, J.; Watts, R. J. *J. Am. Chem. Soc.* **1976**, *98*, 4853–4858.
- (43) Morris, J. V.; Mahaney, M. A.; Huber, J. R. *J. Phys. Chem.* **1976**, *80*, 969–974.

photon counting system (~200 ps resolution) for the time-integrated or time-resolved measurements at room temperature. For the time-resolved measurements, the collected PL was spectrally selected by the spectrometer within a narrow bandwidth (~3 nm) so that only the PL decay at the peaks of maximum emission was monitored. The PL decay was measured at 605 nm for complex **1a**, 600 nm for complexes **1b** and **1c**, 675 and 600 nm for complex **2a** (two maximum PL peaks), and 585 nm for complexes **2b** and **2c**.

Cyclic voltammetry experiments were conducted on an EG&G PAR 263A potentiostat/galvanostat using a three-electrode single compartment cell. A glassy carbon working electrode, a Pt wire auxiliary electrode, and a Ag wire reference electrode were used. For all measurements, samples were dissolved in dimethylformamide (DMF) and degassed with argon. Tetrabutylammonium hexafluorophosphate (Fluka) was used as the supporting electrolyte (0.1 M), and ferrocene (ROC/RIC) was employed as an internal redox reference. All redox potentials are reported *relative* to the ferrocenium/ferrocene (Fc⁺⁰) couple (0.45 V vs SCE⁴⁴ and SCE vs NHE = 0.24 V). All scans were done at 100 millivolts per second unless otherwise noted.

Crystallographic Structure Determinations. Single crystals were attached to glass fibers and mounted under a stream of N₂, maintained at 100.0(1) K, on a Bruker SMART platform diffractometer equipped with an APEX II CCD detector, positioned at -33° in 2θ and 5.0 cm from the samples. The X-ray source, powered at 50 kV and 30 mA, provided Mo Kα radiation (λ = 0.71073 Å, graphite monochromator). Preliminary random samplings of reflections were used to determine unit cells and orientation matrices.⁴⁵ Complete data collections were obtained by ω scans of 183° (0.5° steps) at four different φ settings. Final cell constants were calculated from the xyz centroids of approximately 4000 strong reflections from the actual data collection after integration.⁴⁶ The data were additionally scaled and corrected for absorption.⁴⁷ Space groups were determined based on systematic absences, intensity statistics, and space group frequencies. Structures were solved by direct or Patterson methods.^{48,49} Non-hydrogen atoms were located by difference Fourier syntheses and their positions were refined with anisotropic displacement parameters, unless noted otherwise, by full-matrix least-squares cycles on F².⁴⁸ In a similar fashion all hydrogen atoms were placed geometrically and refined as riding atoms with relative isotropic displacement parameters. The final set of refinement cycles, run to convergence, provided the reported quality assessment parameters.

Materials. K₂PtCl₄ (VWR), methyl 4-formylbenzoate (Fluka), acetophenone (Aldrich), Pd(PPh₃)₄ (Strem), ammonium acetate (EMD), diethyl phosphite (Aldrich), sodium thiophenolate (Fluka), triethylamine (Aldrich), CDCl₃ (Cambridge Isotope Laboratories), and DMSO-*d*₆ (Cambridge Isotope Laboratories) were purchased commercially and used without further purification. 6-Phenyl-4-(4-bromophenyl)-2,2'-bipyridine (**L4**),⁵⁰ 6-phenyl-4-(*p*-tolyl)-2,2'-bipyridine (**L1**),^{29,51} (2-pyridacyl)pyridinium iodide,⁵² *cis*-Pt(DM-

SO)₂Cl₂,⁵³ and [Pt(**L1**)Cl] (**1a**)²⁹ were prepared as reported previously. All other solvents and reagents were purchased commercially and used as received unless otherwise noted.

Synthesis and Characterization of New Ligands and Pt(II) Complexes. **1-Phenyl-3-(4-methylbenzoate)-1-oxoprop-2-ene.** This substrate was made by a previously reported method⁵⁴ from acetophenone (3.76 mmol, 452 mg) and methyl 4-formylbenzoate (3.76 mmol, 617 mg). It was used as isolated. Yield: 392 mg (39%).

6-Phenyl-4-(*p*-methylbenzoate)-2,2'-bipyridine (L2**).** To a flask charged with (2-pyridacyl)pyridinium iodide (1.37 mmol, 446 mg), 1-phenyl-3-(4-methylbenzoate)-1-oxoprop-2-ene (1.37 mmol, 364 mg), and anhydrous ammonium acetate (13.7 mmol, 1.05 g) was added anhydrous MeOH (8 mL) and the mixture was heated to reflux under nitrogen. After ~24 h the suspension was allowed to cool to room temperature (r.t.) and the precipitate was collected by filtration, rinsing with cold MeOH. Yield: 230 mg (45%). MS (APCI): *m/z* 367.2 (M⁺). ¹H NMR (CDCl₃, 400 MHz): δ 8.70 (m, 3H), 8.20 (m, 4H), 8.00 (s, 1H), 7.88 (m, 3H), 7.51 (m, 3H), 7.36 (m, 1H), 3.97 (s, 3H, C[^]N[^]N-Ph-COOCH₃). FT-IR (neat): cm⁻¹ 1709 (ν_{C=O}), 1290 (ν_{C-O}).

6-Phenyl-4-(phenyl-*p*-ethylphosphonate)-2,2'-bipyridine (L3**).** This ligand was prepared by a literature method,⁵⁵ refluxing **L4** (0.41 mmol, 159 mg), diethyl phosphite (0.94 mmol, 0.12 mL), Pd(PPh₃)₄ (0.04 mmol, 47 mg), PPh₃ (4.1 mmol, 1.07 g), and triethylamine (~1 mL) in toluene for 8 h under nitrogen. The product was purified by column chromatography (Silica) eluting with CH₂Cl₂ to remove excess PPh₃, followed by elution with CH₂Cl₂:MeOH (99:1, v/v). In all attempts to isolate pure product, small amounts of triphenylphosphine oxide remained. Even so, the isolated product was used to coordinate to platinum. Yield: 150 mg of 77% pure **L3** (based on ³¹P{¹H} NMR) (63%). ¹H NMR (DMSO-*d*₆, 500 MHz): δ 8.76 (d, 1H, *J* = 3.9 Hz), 8.65 (m, 2H), 8.38 (s, 1H), 8.37 (s, 2H), 8.16 (m, 2H), 8.03 (t, 1H, *J* = 7.2 Hz), 7.91 (m, 2H), 7.57 (m, 4H, overlaps with (O)PPh₃ resonances), 4.07 (m, 4H, C[^]N[^]N-Ph-P(O)(OCH₂CH₃)₂), 1.27 (t, 6H, *J* = 7.0 Hz, C[^]N[^]N-Ph-P(O)(OCH₂CH₃)₂). ³¹P{¹H} NMR (DMSO-*d*₆, 202 MHz): δ 17.34 (s).

[Pt(L2**)Cl] (**1b**).** This complex was prepared by two procedures. The first was a modification of reported methods.^{28,29,56,57} **L2** (0.82 mmol, 300 mg) was suspended in MeCN:MeOH (20 mL, 4:3, v/v) and a solution of K₂PtCl₄ (0.82 mmol, 340 mg) in H₂O (5 mL) was added. The mixture was refluxed under N₂ for ~20 h and allowed to cool to r.t. The orange precipitate was collected by filtration, rinsing with MeOH and Et₂O. Yield: 208 mg (43%).

For the second method of preparation, **L2** (0.14 mmol, 50 mg) was dissolved in a small amount of CHCl₃ (~5 mL) and *cis*-Pt(DMSO)₂Cl₂ (0.17 mmol, 70 mg) was added, and the mixture was heated to reflux for ~24 h under nitrogen. The orange precipitate was collected by filtration, rinsing with cold CHCl₃ and Et₂O. Yield: 68 mg (82%). MS (APCI): *m/z* 596.1 (M⁺). ¹H NMR (DMSO-*d*₆, 500 MHz): δ 8.96 (d, 1H, *J* = 4.7 Hz), 8.80 (d, 1H, *J* = 8.0 Hz), 8.61 (s, 1H), 8.41 (m, 2H), 8.29 (d, 2H, *J* = 8.1 Hz),

(44) Connelly, N. G.; Geiger, W. E. *Chem. Rev.* **1996**, *96*, 877–910.

(45) APEX2, V2.1–0; Bruker AXS: Madison, WI, 2006.

(46) SAINT, V7.34A; Bruker AXS: Madison, WI, 2006.

(47) Sheldrick, G. M. *SADABS*, V2004/1, University of Göttingen: Göttingen, Germany, 2004.

(48) SHELXTL, V6.14; Bruker AXS: Madison, WI, 2000.

(49) Altomare, A.; Burla, M. C.; Camalli, M.; Cascarano, G. L.; Giacovazzo, C.; Guagliardi, A.; Moliterni, A. G. G.; Polidori, G.; Spagna, R. *SIR97: A New Program for Solving and Refining Crystal Structures*; Istituto di Cristallografia, CNR: Bari, Italy, 1999.

(50) Schmelz, O.; Rehahn, M. *e-Polym.* **2002**, *47*; no pp given.

(51) Neve, F.; Crispini, A.; Campagna, S.; Serroni, S. *Inorg. Chem.* **1999**, *38*, 2250–2258.

(52) Ballardini, R.; Balzani, V.; Clemente-Leon, M.; Credi, A.; Gandolfi, M. T.; Ishow, E.; Perkins, J.; Stoddart, J. F.; Tseng, H.-R.; Wenger, S. *J. Am. Chem. Soc.* **2002**, *124*, 12786–12795.

(53) Kukushkin, V. Y.; Pombeiro, A. J. L.; Ferreira, C. M. P.; Elding, L. I.; Puddephatt, R. J. *Inorg. Synth.* **2002**, *33*, 189–196.

(54) Mukkala, V. M.; Helenius, M.; Hemmila, I.; Kankare, J.; Takalo, H. *Helv. Chim. Acta* **1993**, *76*, 1361–1378.

(55) Penicaud, V.; Odobel, F.; Bujoli, B. *Tetrahedron Lett.* **1998**, *39*, 3689–3692.

(56) Constable, E. C.; Henney, R. P. G.; Leese, T. A.; Tocher, D. A. *J. Chem. Soc., Chem. Commun.* **1990**, 513–515.

(57) Neve, F.; Crispini, A.; Campagna, S. *Inorg. Chem.* **1997**, *36*, 6150–6156.

8.16 (d, 2H, $J = 8.3$ Hz), 7.97 (t, 1H, $J = 6.7$ Hz), 7.87 (d, 1H, $J = 7.0$ Hz), 7.54 (d, 1H, $J = 7.9$ Hz), 7.19 (t, 1H, $J = 7.3$ Hz), 7.12 (t, 1H, $J = 6.7$ Hz), 3.93 (s, 3H, C^{^N^N}-Ph-COOCH₃). FT-IR (neat): cm⁻¹ 1730 ($\nu_{C=O}$), 1279 (ν_{C-O}). Anal. Calcd for C₂₄H₁₇ClN₂O₂Pt: C, 48.37; H, 2.88; N, 4.70. Found: C, 47.78; H, 2.72; N, 4.62.

[Pt(L3)Cl] (1c). This compound was prepared in the same manner as the first method for **1b**, using **L3** (0.33 mmol, 150 mg) in place of **L2**, with K₂PtCl₄ (0.33 mmol, 140 mg). After refluxing for ~20 h, the solvent was removed under vacuum. To the orange residue was added a small amount of MeOH (2 mL), and after a few minutes the orange precipitate was collected by filtration, rinsing with Et₂O. Yield: 81 mg (46%). MS (APCI): m/z 674.1 (M⁺). ¹H NMR (DMSO-*d*₆, 500 MHz): δ 8.95 (d, 1H, $J = 4.3$ Hz), 8.77 (d, 1H, $J = 7.8$ Hz), 8.59 (s, 1H), 8.41 (t, 1H, $J = 7.4$ Hz), 8.36 (s, 1H), 8.27 (d, 2H, $J = 4.8$ Hz), 7.93 (m, 3H), 7.85 (d, 1H, $J = 7.3$ Hz), 7.53 (d, 1H, $J = 7.4$ Hz), 7.19 (t, 1H, $J = 7.3$ Hz), 7.12 (t, 1H, $J = 7.2$ Hz), 4.08 (m, 4H, C^{^N^N}-Ph-P(O)(OCH₂CH₃)₂), 1.28 (t, 6H, $J = 7.0$ Hz, C^{^N^N}-Ph-P(O)(OCH₂CH₃)₂). ³¹P{¹H} NMR (DMSO-*d*₆, 202 MHz): δ 17.07 (s). FT-IR (neat): cm⁻¹ 1240 ($\nu_{P=O}$). Anal. Calcd for C₂₆H₂₄ClN₂O₃PPt: C, 46.33; H, 3.59; N, 4.16. Found: C, 41.52; H, 3.48; N, 4.46.

[Pt(L1)(SPh)] (2a). To a suspension of **1a** (0.072 mmol, 41 mg) in MeOH (10 mL) was added a solution of sodium thiophenolate (0.083 mmol, 12 mg) in H₂O:MeOH (2:1, v/v) (10 mL). The mixture was purged with N₂ for several minutes and allowed to stir at r.t. for ~3 days, or until the mixture became dark blue/green. Volatile solvent was removed under vacuum, and the dark solid was isolated by centrifuge, rinsing with H₂O and a small amount of MeOH, until thiolate smell had dissipated. The dark colored product was dried under vacuum and was recrystallized by slow diffusion of Et₂O into a CH₂Cl₂ solution of the product. The recrystallized product was collected by filtration and stored under nitrogen. Yield: 37 mg (82%). MS (APCI): m/z 626.1 (M⁺). ¹H NMR (DMSO-*d*₆, 500 MHz): δ 8.78 (d, 1H, $J = 7.9$ Hz), 8.61 (s, 1H), 8.52 (d, 1H, $J = 6.1$ Hz), 8.38 (s, 1H), 8.32 (t, 1H, $J = 7.5$ Hz), 8.09 (d, 2H, $J = 7.9$ Hz), 7.89 (d, 1H, 6.4 Hz), 7.66 (t, 1H, $J = 6.6$ Hz), 7.54 (m, 3H), 7.44 (d, 2H, $J = 7.7$ Hz), 7.07 (m, 2H), 6.99 (t, 2H, $J = 7.4$ Hz), 6.88 (t, 1H, $J = 7.1$ Hz), 2.42 (s, 3H, C^{^N^N}-Ph-CH₃). Anal. Calcd for C₂₉H₂₂N₂SPT: C, 55.67; H, 3.54; N, 4.48. Found: C, 54.50; H, 3.36; N, 4.50.

[Pt(L2)(SPh)] (2b). To a solution of **1b** (0.047 mmol, 28 mg) in CH₂Cl₂ (25 mL) was added a suspension of sodium thiophenolate (0.052 mmol, 7 mg) in MeOH (5 mL). The dark purple mixture was purged with N₂ and allowed to stir at r.t. for ~2 days after which the solvent was removed under vacuum, and the residue was resuspended in MeOH:H₂O (1:5, v/v), isolated by centrifuge, rinsing with H₂O and MeOH until thiolate smell had dissipated. The dark purple product was purified by column chromatography (neutral Alumina) eluting with CH₂Cl₂ followed by MeCN. The recovered product was redissolved in CH₂Cl₂ and addition of Et₂O caused a dark purple precipitate to crash out. The product was collected by filtration and stored under nitrogen. Yield: 14 mg (45%). MS (APCI): m/z 670.2 (M⁺). ¹H NMR (DMSO-*d*₆, 400 MHz): δ 8.78 (d, 1H, $J = 7.6$ Hz), 8.68 (s, 1H), 8.49 (d, 1H, $J = 4.5$ Hz), 8.46 (s, 1H), 8.31 (d, 3H, $J = 7.7$ Hz), 8.16 (d, 2H, $J = 7.8$ Hz), 7.91 (m, 1H), 7.67 (t, 1H), 7.55 (d, 3H, $J = 7.7$ Hz), 7.08 (m, 2H), 7.00 (t, 2H, $J = 7.4$ Hz), 6.90 (t, 1H), 3.93 (s, 3H, C^{^N^N}-Ph-COOCH₃).

FT-IR (neat): cm⁻¹ 1713 ($\nu_{C=O}$), 1273 (ν_{C-O}). Anal. Calcd for C₃₀H₂₂N₂O₂SPT: C, 53.80; H, 3.31; N, 4.18. Found: C, 53.75; H, 3.52; N, 3.86.

[Pt(L3)(SPh)] (2c). This compound was prepared by the same method as for **2a**, using **1c** (0.074 mmol, 50 mg) in place of **1a**, with sodium thiophenolate (0.087 mmol, 12 mg). Final recovered product stored under nitrogen. Yield: 42 mg (76%). MS (APCI): m/z 748.2 (M⁺). ¹H NMR (DMSO-*d*₆, 500 MHz): δ 8.76 (d, 1H, $J = 7.8$ Hz), 8.66 (s, 1H), 8.51 (d, 1H, $J = 4.9$ Hz), 8.44 (s, 1H), 8.31 (m, 3H), 7.93 (m, 3H), 7.67 (t, 1H, $J = 6.2$ Hz), 7.55 (d, 3H), 7.09 (m, 2H), 7.00 (t, 2H, $J = 7.5$ Hz), 6.89 (t, 1H, 7.3 Hz), 4.09 (m, 4H, C^{^N^N}-Ph-P(O)(CH₂CH₃)₂), 1.28 (t, 6H, $J = 7.0$ Hz, C^{^N^N}-Ph-P(O)(CH₂CH₃)₂). ³¹P{¹H} NMR (DMSO-*d*₆, 202 MHz): δ 17.12 (s). FT-IR (neat): cm⁻¹ 1250 ($\nu_{P=O}$). Anal. Calcd for C₃₂H₂₆N₂O₃PSPT: C, 51.40; H, 3.91; N, 3.75. Found: C, 51.11; H, 3.81; N, 3.74.

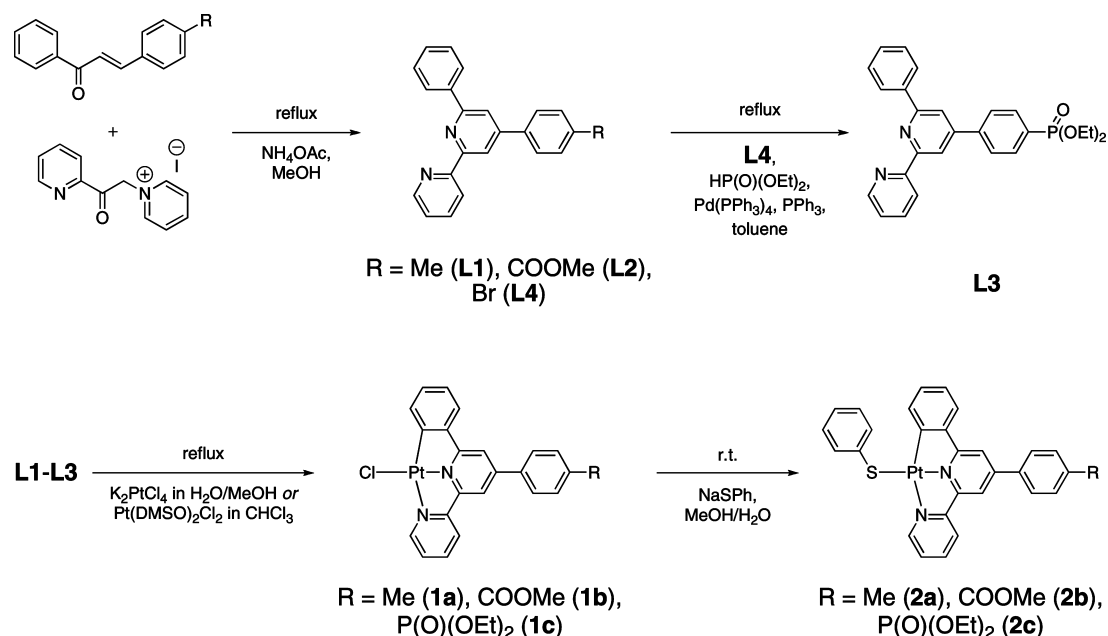
Results and Discussion

Synthesis and Characterization. The substituted 6-phenyl-4-(*p*-R-phenyl)-2,2'-bipyridine ligands (R = Me (**L1**), COOMe (**L2**), and Br (**L4**)) were made from a modification of the Kröhnke pyridine synthesis that involves heating a methanol mixture of the appropriate (*E*)-propenone and pyridinium iodide substrates in the presence of ammonium acetate (Scheme 1).^{54,58} For R = P(O)(OEt)₂ (**L3**), the aryl phosphonate was made by a Pd catalyzed phosphonation of **L4** with diethylphosphite, using Pd(PPh₃)₄ as the Pd source and ~10 fold excess PPh₃.⁵⁵ The resulting ligands **L1–L3** were then allowed to react with K₂PtCl₄ or Pt(DMSO)₂Cl₂ using a combination of known procedures to give the neutral cyclometalated Pt C^{^N^N} chloride complexes **1a**, **1b**, and **1c**, respectively (Scheme 1).^{28,29,56,57} It was found that using Pt(DMSO)₂Cl₂ as the Pt(II) source nearly doubled the yields of **1a–1c**. Facile displacement of the chloride by thiophenolate occurred from stirring a MeOH mixture of **1a–1c** with an aqueous solution of sodium thiophenolate under nitrogen, giving complexes **2a**, **2b**, and **2c**, respectively, in high yields (Scheme 1). The new ligands and complexes have been characterized by various methods that include ¹H and ³¹P NMR spectroscopies, mass spectrometry, FT-IR spectroscopy, elemental analysis, and single crystal X-ray diffraction. The elemental analysis for complex **1c** is not satisfactory; the low percent carbon is due in part to difficulties getting complete combustion of the complex under experimental conditions.

Crystal Structure Determinations. Crystals suitable for single crystal X-ray diffraction were obtained for ligand **L2** and metal complexes **1a**, **1b**, and **2b**. The unit cell, data collection and refinement parameters are located in Table 1, with selected bond lengths and angles summarized in Table 2. Crystals of **2b** were obtained by the slow diffusion of diethyl ether into a CH₂Cl₂ solution of the complex (Figure 1). There are two independent Pt molecules in the asymmetric unit, with two co-crystallized CH₂Cl₂ solvent molecules per Pt complex, one of which is disordered over a crystallographic inversion center (50:50). The molecule containing Pt(1) has a C:N disorder (52:48) at the Pt(C^{^N^N}) core; the

(58) Kröhnke, F. *Synthesis* **1976**, 1–24.

Scheme 1

**Table 1.** Crystallographic Data and Structure Refinement for Ligand **L2** and Complexes **1a**·MeCN, **1b**, and **2b**·CH₂Cl₂

	L2	1a ·MeCN	1b	2b ·CH ₂ Cl ₂
formula	C ₂₄ H ₁₈ N ₂ O ₂	C ₂₅ H ₂₀ Cl _{0.89} I _{0.11} N ₃ Pt	C ₂₄ H ₁₇ ClN ₂ O ₂ Pt	C ₃₂ H ₂₄ Cl ₂ N ₂ O ₂ PtS
Fw	366.40	602.58	595.94	754.57
<i>T</i> (K)	100.0(1)	100.0(1)	100.0(1)	100.0(1)
λ (Å)	0.71073	0.71073	0.71073	0.71073
crystal system	orthorhombic	orthorhombic	monoclinic	triclinic
space group	<i>Pbcn</i>	<i>Pnma</i>	<i>P2₁/n</i>	<i>P</i> $\bar{1}$
<i>a</i> (Å)	28.8215(18)	13.315(3)	7.209(3)	7.5080(9)
<i>b</i> (Å)	6.9172(4)	6.6392(17)	17.849(8)	16.2851(19)
<i>c</i> (Å)	18.2398(11)	23.221(6)	30.341(14)	23.239(3)
α (deg)	90	90	90	81.577(2)
β (deg)	90	90	93.407(6)	89.130(2)
γ (deg)	90	90	90	89.437(2)
<i>V</i> (Å ³)	3636.4(4)	2052.7(9)	3897(3)	2810.3(6)
<i>Z</i>	8	4	8	4
ρ_{calc} (Mg/m ³)	1.339	1.950	2.031	1.783
μ (mm ⁻¹)	0.086	7.128	7.363	5.290
crystal color	colorless plate	orange needle	orange needle	red-black plate
crystal size (mm ³)	0.50 × 0.36 × 0.08	0.45 × 0.12 × 0.06	0.22 × 0.03 × 0.01	0.24 × 0.22 × 0.04
θ range (deg)	2.23–32.56	1.75–32.56	1.76–25.02	1.43–32.03
no. of data	6608	3979	6897	19323
no. of parameters	325	184	261	716
GOF ^a	1.044	1.083	1.046	1.036
<i>R1</i> , <i>wR2</i> (<i>F</i> ² , <i>I</i> > 2 σ (<i>I</i>)) ^b	0.0427, 0.1103	0.0222, 0.0450	0.0970, 0.1805	0.0466, 0.1133
<i>R1</i> , <i>wR2</i> (<i>F</i> ² , all data) ^b	0.0513, 0.1173	0.0295, 0.0470	0.2141, 0.2243	0.0727, 0.1234

^a GOF = $S = \sum w(F_o^2 - F_c^2)^2 / (m - n)^{1/2}$, where *m* = number of reflections and *n* = number of parameters. ^b $R1 = \sum |F_o| - |F_c| / \sum |F_o|$, $wR2 = [\sum w(F_o^2 - F_c^2)^2]^{1/2} / \sum w(F_o^2)^{1/2}$, where $w = 1/[\sigma^2(F_o^2) + (aP) + bP]$ and $P = \sum \max(0, F_o^2) + 2/3 F_c^2$.

molecule containing Pt(2) has its thiophenolate modeled as disordered over two positions (50:50). π -stacking of the central C[^]N[^]N[^] coordination sphere is observed between pairs of molecules (~3.3 Å). To the best of our knowledge there are no literature reports for the structural characterization of Pt(II) (C[^]N[^]N[^]) thiolate complexes, and there are few accounts of Pt(II) complexes with a coordination sphere that contains an anionic carbon, a thiolate, and two neutral N-donors. Ma et al.⁵⁹ and Koshiyama et al.⁶⁰ have structurally characterized cyclometalated dinuclear Pt(II) complexes

of the general formula, [Pt₂(ppy)₂(pyt)₂] (ppy = 2-phenylpyridine, pyt = pyridine-2-thiol), that are bridged by pyridine-2-thiolate. Moreover, there is only one reported structure of a platinum thiophenolate complex, the cationic Pt(IV) octahedral species [PtMe₂(SPh)(PEt₃)(dbbpy)]⁺ (dbbpy = 4,4'-di-*tert*-butyl-2,2'-bipyridine).⁶¹

Slow evaporation of a CH₂Cl₂/MeCN solution of **1a** yielded long orange needles suitable for single crystal X-ray diffraction. There is a halogen (chloride:iodide) site oc-

(59) Ma, B.; Djurovich, P. I.; Garon, S.; Alleyne, B.; Thompson, M. E. *Adv. Funct. Mater.* **2006**, *16*, 2438–2446.

(60) Koshiyama, T.; Ai, O.; Kato, M. *Chem. Lett.* **2004**, *33*, 1386–1387.

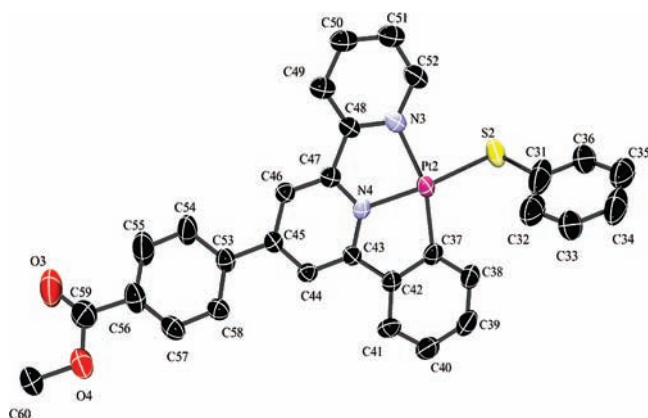
(61) Janzen, M. C.; Jennings, M. C.; Puddephatt, R. J. *Can. J. Chem.* **2002**, *80*, 41–45.

(62) It is presumed that the iodide present remains from the synthesis of the L1 ligand.

Table 2. Selected Bond Lengths (Å) and Angles (deg) for Ligand **L2**, and Complexes **1a**·MeCN, **1b**, and **2b**·CH₂Cl₂

Ligand L2			
C(4)–C(5)–C(6)–N(2)	12.00(12)	C(7)–C(8)–C(17)–C(22)	21.14(12)
N(2)–C(10)–C(11)–C(12)	22.65(11)		
Complex 1a ·MeCN			
Pt(1)–N(1)	1.954(3)	Pt(1)–C(1)	1.993(3)
Pt(1)–N(2)	2.109(3)	Pt(1)–Cl(1) ^a	2.3657(7)
N(1)–Pt(1)–N(2)	79.31(11)	C(1)–Pt(1)–N(2)	161.38(12)
N(1)–Pt(1)–C(1)	82.08(12)	N(1)–Pt(1)–Cl(1) ^a	179.25(8)
C(10)–C(9)–C(17)–C(22)	0.000(2)		
Complex 1b ^b			
Pt(1)–Cl(1)	2.323(7)	Pt(2)–Cl(2)	2.307(7)
Complex 2b ·CH ₂ Cl ₂ ^c			
Pt(1)–N(2)	1.984(4)	Pt(2)–N(4)	1.977(4)
Pt(1)–N(1)	2.062(5)	Pt(2)–N(3)	2.104(5)
Pt(1)–C(7)	2.061(4)	Pt(2)–C(37)	1.998(6)
Pt(1)–S(1)	2.994(13)	Pt(2)–S(2) ^d	2.298
N(2)–Pt(1)–N(1)	80.09(17)	N(4)–Pt(2)–N(3)	79.25(18)
N(2)–Pt(1)–C(7)	80.17(17)	N(4)–Pt(2)–C(37)	82.1(2)
C(7)–Pt(1)–N(1)	160.22(18)	C(37)–Pt(2)–N(3)	161.4(2)
N(2)–Pt(1)–S(1)	178.45(11)	N(4)–Pt(2)–S(2) ^d	174.1
C(7)–Pt(1)–S(1)–C(1)	53.3(2)	C(37)–Pt(2)–S(2)–C(31) ^d	73.1
C(14)–C(15)–C(23)–C(24)	39.7(7)	C(46)–C(45)–C(53)–C(54)	37.0(9)

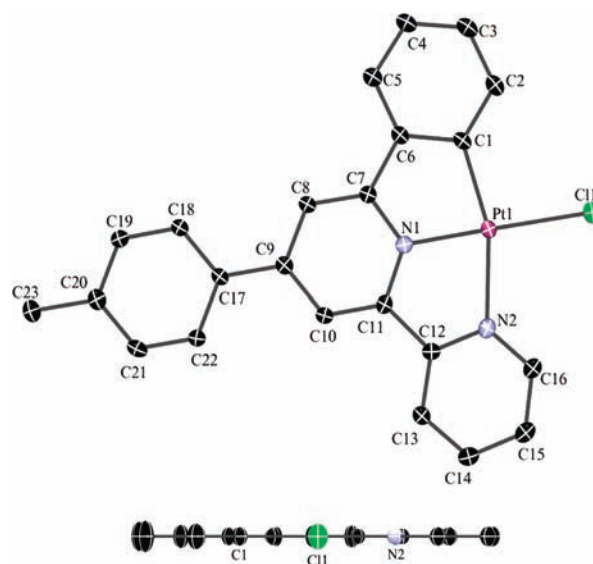
^a There is a halogen (chloride:iodide) site occupancy disorder of 89:11 (Cl:I).⁶² ^b There are two unique molecules per asymmetric unit, but only the Pt and Cl atoms were refined with anisotropic displacement parameters. ^c There are two unique molecules per asymmetric unit. ^d Thiophenolate modeled as disordered over two positions (50:50), values reported are an average of the two.

**Figure 1.** ORTEP drawing of one of the unique molecules of complex **2b**·CH₂Cl₂.

cupancy disorder of 89:11 (Cl:I),⁶² and since the disordered atoms were refined isopositionally, the bond length is based on the percentage of each component. Though it is roughly 10% iodide in character, the Pt(1)–Cl(1) bond distance of 2.3657(7) Å is only slightly elongated (~0.05 Å) compared to Pt–Cl distances reported for similar [Pt(C^{^N}N)Cl] complexes: 2.312(2), 2.307(2), and 2.316(2) Å for [Pt(pbpy)Cl] where pbpy = 6-phenyl-2,2'-bipyridine;⁶³ 2.319(4) Å for [Pt(4-(aza-15-crown-5)-pbpy)Cl];⁶⁴ and 2.302(2) Å for [Pt(4'-(4-dodecyloxy)phenyl)-pbpy)Cl].⁵⁷ Complex **1a** and one MeCN solvent molecule lie on crystallographic mirror planes, shown in Figure 2 without the MeCN. There are no observed Pt–Pt interactions since the nearest Pt···Pt distance is 5.693 Å; however, there is π -stacking (~3.33 Å) between the bipyridyl parts of C^{^N}N ligands of adjacent molecules.

(63) Hofmann, A.; Dahlenburg, L.; van Eldik, R. *Inorg. Chem.* **2003**, *42*, 6528–6538.

(64) Lu, W.; Chan, M. C. W.; Zhu, N.; Che, C.-M.; Li, C.; Hui, Z. *J. Am. Chem. Soc.* **2004**, *126*, 7639–7651.

**Figure 2.** ORTEP drawings of complex **1a**·MeCN. Looking down the Cl–Pt bond, the bottom drawing shows the planarity of the pendant tolyl group with the Pt(C^{^N}N) core.

They are aligned in such a manner that the cyclometalated phenyl ring is not participating in π -stacking interactions. The orientation of the pendant phenyl ring is also noteworthy, as it is planar with the cyclometalated portion of the C^{^N}N ligand (Figure 2, bottom). This observation is atypical for these types of ligands and is not the case for the pendant ring in crystal structures of **L2**, **1b**, and **2b**.

Crystals of **1b** were grown by the slow evaporation of a concentrated CH₂Cl₂ solution. There are two unique molecules per asymmetric unit, but only the Pt and Cl atoms were refined with anisotropic displacement parameters; all other atoms could not be refined anisotropically. This structure is informative for connectivity only, and the bond lengths and angles reported, other than the Pt–Cl distances,

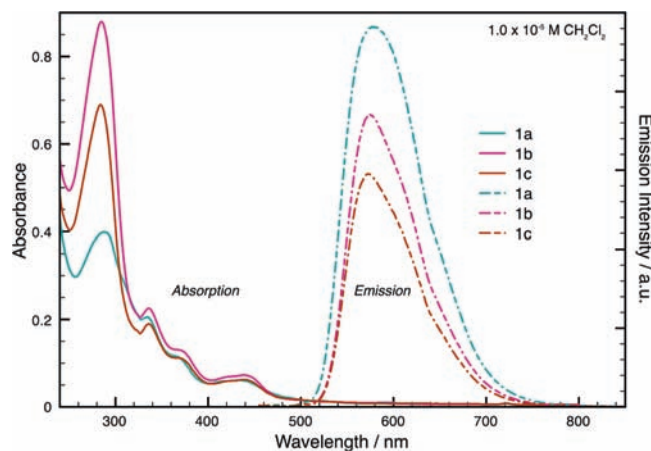


Figure 3. Steady-state room temperature absorption and emission ($\lambda_{\text{ex}} = 435$ nm) spectra of complexes **1a–1c** in CH_2Cl_2 solution.

are intended as mere guidelines. The Pt–Cl distances in **1b** were found to be 2.323(7) Å for Pt(1)–Cl(1) and 2.307(7) Å for Pt(2)–Cl(2); these values compare well with Pt–Cl distances reported for analogous [Pt(C^{^N}^{^N})Cl] structures.^{57,63,64}

Electronic Absorption Spectroscopy. The electronic spectra of **1b** and **1c** in CH_2Cl_2 fluid solution are very similar to that of **1a**, which has been discussed elsewhere.⁶⁵ Figure 3 shows that the UV region of the spectrum ($\lambda < 370$ nm) is dominated by intraligand (IL) transitions with molar absorptivities (ϵ) that range from ~ 8500 – $24,000$ $\text{dm}^3 \text{mol}^{-1} \text{cm}^{-1}$. There is a maximum at about 285 nm, and there are two additional shoulders near 335 and 370 nm. Another lower energy maximum centered around 440 nm ($\epsilon \sim 4800$ $\text{dm}^3 \text{mol}^{-1} \text{cm}^{-1}$) and ending just beyond 500 nm has been assigned to a metal-to-ligand charge-transfer (¹MLCT) transition.^{29,57}

Like their precursors in CH_2Cl_2 fluid solution, complexes **2a**, **2b**, and **2c** exhibit IL transitions in the UV region of their electronic spectra with maxima at about 285 nm and shoulders around 330 and 370 nm with molar absorptivities ranging between $\sim 10,500$ – $33,500$ $\text{dm}^3 \text{mol}^{-1} \text{cm}^{-1}$. In the visible region, the absorption bands at 411, 418, and 415 nm for **2a**, **2b**, and **2c**, respectively, are tentatively assigned to a $d\pi(\text{Pt})/p$ (thiophenolate) $\rightarrow \pi^*$ (C^{^N}^{^N} ligand) charge-transfer (¹CT) transition, while a second absorption band of slightly greater magnitude ($\epsilon \sim 4000$ $\text{dm}^3 \text{mol}^{-1} \text{cm}^{-1}$) is observed at 551, 560, and 560 nm, respectively (Figure 4). While the ¹CT transition at 411–418 nm varies only slightly (~ 5 nm) with solvent, the lower energy bands observed for complexes **2a–2c** at 551–560 nm are solvent dependent and are likely charge-transfer (CT) in nature,²² an assignment discussed further in the solvatochromism section of the paper.

Electrochemistry. The electrochemical behavior of ligands **L1** and **L2** and complexes **1a–1c** and **2a–2c** has been examined by cyclic voltammetry, and the data are summarized in Table 3, with cyclic voltammograms for all complexes available in the Supporting Information. All of the redox potentials are reported relative to NHE with the

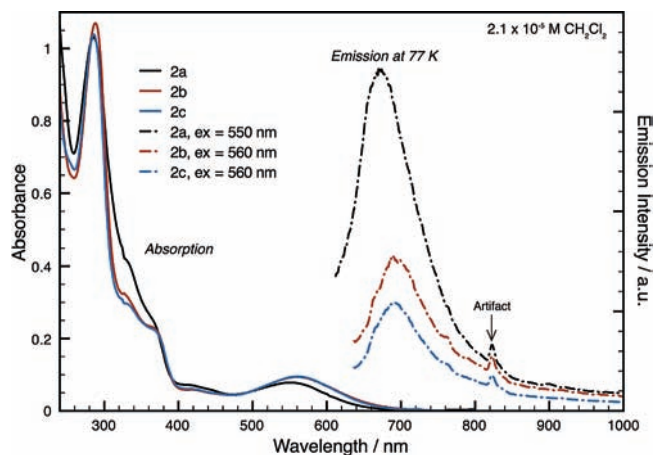


Figure 4. Room temperature absorption and 77 K emission spectra of complexes **2a–2c** in CH_2Cl_2 solution.

Table 3. Electrochemical Potentials for Ligands **L1** and **L2** and Complexes **1a–1c** and **2a–2c**, As Determined by Cyclic Voltammetry^a

complex/ligand	reduction $E^{1/2}/\text{V}$	oxidation ^b E/V
L1	–1.81	
L2	–1.46	
1a	–1.04, –1.66	+1.10
1b	–0.98, –1.48	+1.10
1c	–0.98, –1.54	+1.14
2a	–1.06, –1.67	+1.29 ^c , +1.51 ^c
2b	–0.98, –1.46	+1.29 ^d , +1.53 ^d
2c	–1.00, –1.51	+1.34 ^e

^a All redox potentials are reported versus NHE relative to the $\text{Fc}^{+/0}$ couple (0.45 V vs SCE⁴⁴ and SCE vs NHE = 0.24 V). ^b All oxidations are irreversible under experimental conditions. ^c 500 mV/sec scan rate. ^d 300 mV/sec scan rate. ^e 500 mV/sec scan rate; only one observed oxidation.

ferrocenium/ferrocene ($\text{Fc}^{+/0}$) couple used as an internal redox standard and a value of 0.45 V versus SCE taken for the $\text{Fc}^{+/0}$ couple,⁴⁴ and a value of 0.24 V taken for SCE versus NHE. The ligands show one quasi-reversible reduction at –1.81 and –1.46 V (vs NHE) for **L1** and **L2**, respectively. Ligand **L2** is easier to reduce than **L1** because of the electron withdrawing nature of the pendant R = COOMe group. For **1a–1c** there are two reductions that reside on the coordinated C^{^N}^{^N} ligand for each complex with potential values of –1.04, –0.98, and –0.98 V for the first reduction and –1.66, –1.48, and –1.54 V for the second reduction for **1a**, **1b**, and **1c**, respectively. That complexes **1b** and **1c** are only slightly easier to reduce than **1a** suggests the electron withdrawing nature of the pendant groups in **1b** and **1c** relative to that of **1a** are exerting only a minimal electronic effect on the C^{^N}^{^N} ligand, possibly because of the intervening *p*-phenylene group which is twisted relative to the central pyriding ring of the ligand. Complexes **2a–2c** also show two reductions with potentials of –1.06, –0.98, and –1.00 V for the first reduction and –1.67, –1.46, and –1.51 V for the second reduction for **2a**, **2b**, and **2c**, respectively. Like their chloride precursors, the thiophenolate complexes with electron withdrawing ester groups on the C^{^N}^{^N} ligands are only slightly easier to reduce than the R = Me analogue. A previous study for a series of [(C^{^N}^{^N})PtC≡CR] complexes reported only one observed reduction in CH_2Cl_2 solution,²⁸ possibly because of a different solvent window than for the current study, which was done in DMF.

(65) Cheung, T.-C.; Cheung, K.-K.; Peng, S.-M.; Che, C.-M. *J. Chem. Soc., Dalton Trans.* **1996**, 1645–1651.

Table 4. Spectroscopic and Photophysical Data for Complexes **1a–1c** in 1.0×10^{-5} M CH_2Cl_2 Solution at Room Temperature

	$\lambda_{\text{abs}}/\text{nm}$ ($\epsilon/\text{dm}^3 \text{ mol}^{-1} \text{ cm}^{-1}$)	solution $\lambda_{\text{em}}^{\text{max}}/\text{nm}^a$	τ/ns^b	$\phi_{\text{em}}^{a,c}$
1a	291 (20 040), 336 (14 580), 368 (8460), 436 (4440)	577, 640 (sh)	580	0.066
1b	288 (24 160), 336 (15 410), 369 (9220), 440 (4940)	574, 610 (sh), 640 (sh)	390	0.038
1c	285 (19 560), 336 (14 770), 367 (8880), 439 (4640)	573, 610 (sh), 640 (sh)	385	0.035

^a $\lambda_{\text{ex}} = 435$ nm; sh = shoulder. ^b $\lambda_{\text{ex}} = 450$ nm. ^c Emission quantum yields (ϕ_{em}) measured relative to $\text{Ru}(\text{bpy})_3\text{Cl}_2$ in H_2O ($\phi_{\text{em}} = 0.042$).⁴²

Table 5. Spectroscopic and Photophysical Data for Complexes **2a–2c** in 2.1×10^{-5} M CH_2Cl_2

	$\lambda_{\text{abs}}/\text{nm}$ ($\epsilon/\text{dm}^3 \text{ mol}^{-1} \text{ cm}^{-1}$)	soln $\lambda_{\text{em}}^{\text{max}}/\text{nm}^a$	τ/ns^b	ϕ_{em}^c	77 K soln $\lambda_{\text{em}}^{\text{max}}/\text{nm}$
2a	286 (30 770), ~330 (17 770), ~370 (10 650), 411 (3220), 551 (3440)	570; 566; 564	135, 235	0.016; 0.049	672 ^d
2b	288 (33 560), ~330 (15 220), ~370 (11 350), 418 (3190), 560 (4690)	544, 570 (sh); 545, 570 (sh); 562	230	0.003; 0.011	694 ^e
2c	286 (29 730), ~330 (13 960), ~370 (10 570), 415 (2950), 560 (4130)	566; 559; 563	305	0.002; 0.002	692 ^e

^a $\lambda_{\text{ex}} = 410$ nm; 370 nm; 335 nm; sh = shoulder. ^b $\lambda_{\text{ex}} = 403$ nm; for complex **2a**, the emission lifetime was measured for two different maxima. ^c Emission quantum yields ($\lambda_{\text{ex}} = 335$ nm; 410 nm) measured relative to $\text{Ru}(\text{bpy})_3\text{Cl}_2$ in H_2O ($\phi_{\text{em}} = 0.042$).⁴² ^d $\lambda_{\text{ex}} = 550$ nm. ^e $\lambda_{\text{ex}} = 560$ nm.

Neither **L1** or **L2** display an oxidation, but for complexes **1a–1c** there is an irreversible oxidation observed at +1.10, +1.10, and +1.14 V (vs NHE), respectively, that has tentatively been assigned to a $\text{Pt}^{\text{II/III}}$ oxidation process.¹³ In addition, the oxidation potentials for **2a–2c** at +1.29, +1.29, and +1.34 V, respectively, are also speculated to be a $\text{Pt}^{\text{II/III}}$ oxidation process. Though they are difficult to discern, complexes **2a** and **2b** display an additional irreversible oxidation wave at +1.51 and +1.53 V, respectively, which has tentatively been assigned to an oxidation of the thiophenolate ligand. This second oxidation was not observed for complex **2c**.

Steady-State and Frozen Emission Spectra. The absorption and emission data for complexes **1a–1c** and **2a–2c** are summarized in Tables 4 and 5. The chloro complexes **1a**, **1b**, and **1c** are emissive in fluid solution with λ_{max} at 577, 574, and 573 nm, respectively, when $\lambda_{\text{ex}} = 435$ nm (Figure 3), and have quantum yields (ϕ_{em}) of 0.066, 0.038, and 0.035, respectively, measured relative to $\text{Ru}(\text{bpy})_3\text{Cl}_2$ in H_2O .⁴² The luminescence lifetimes range between 385–580 ns, leading to assignment of the excited state as a ³MLCT transition.²⁹ Similar to what was observed electrochemically for complexes **1a–1c**, the electron withdrawing nature of the ester groups in **1b** and **1c** exert little effect on the lowest unoccupied π^* orbital localized on the $\text{C}^{\wedge}\text{N}^{\wedge}\text{N}$ ligands, as the difference in maximum emission between complexes is not significant.

When complexes **2a–2c** are excited into the lower energy CT band ($\lambda_{\text{ex}} = 550$ nm for **2a**, $\lambda_{\text{ex}} = 560$ nm for **2b** and **2c**) there is no emission in fluid solution; however, they are emissive in frozen CH_2Cl_2 solution with λ_{max} of 672, 694, and 692 nm, respectively (Figure 4). The electron withdrawing ester groups in **2b** and **2c** appear to have a similar effect, slightly shifting the CT emission by ~20 nm compared to the emission of **2a**.

Complexes **2a–2c** are emissive in fluid CH_2Cl_2 when excited at $\lambda \leq 410$ nm, and the respective emission maxima are nearly the same regardless of the excitation wavelength (Table 5, Supporting Information, Figure S4). Complexes **2a** and **2c** show broad structureless emissions with λ_{max} that range between 559 and 570 nm whereas complex **2b**, when excited at 410 or 370 nm, exhibits narrower emission maxima at about 545 nm with shoulders at ~570 nm. When excited at 335 nm, complex **2b** exhibits a broader emission profile

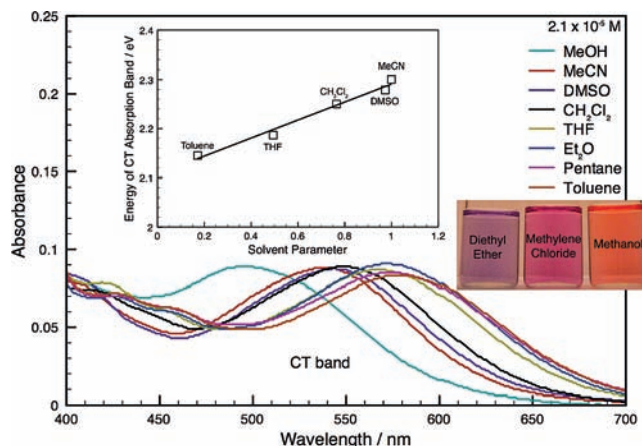


Figure 5. Steady-state room temperature absorption spectra of complex **2a** in different solvents. Insets: Plot of the maximum absorption energy of the MMLL/CT transition (eV) versus empirical Solvent Parameter values; and a photograph of solutions of **2a** in diethylether, methylene chloride, and methanol.

like that of **2a** and **2c**, with an emission maximum centered at 563 nm. There are only subtle differences in the emission maxima between complexes. The luminescence lifetimes for exciting complexes **2b** and **2c** at 403 nm are 230 and 305 ns, respectively. When measuring the photoluminescent decay of complex **2a** at 403 nm excitation, there were two observed emission maxima, one having a lifetime of 135 ns and the other a slightly longer lifetime of 235 ns. On the basis of the lifetime measurements, the observed emission for complexes **2a–2c** excited at 403 nm are assigned to a charge-transfer to $\text{C}^{\wedge}\text{N}^{\wedge}\text{N}$ (³CT) emissive state, which we think has the same LUMO as suggested for **1a–1c** but possesses a different HOMO.

Solvatochromism. Further investigation of the lower energy CT absorption maxima at 551, 560, and 560 nm for complexes **2a**, **2b**, and **2c**, respectively, shows evidence that the CT bands are solvatochromic. For complex **2a** the lower energy CT absorption ranges between 496 nm in MeOH to 578 nm in toluene (see Figure 5). The photograph in Figure 5 shows the distinct color change of **2a** from pink in MeOH to purple in CH_2Cl_2 to blue in diethyl ether. Complexes **2b** and **2c** display similar solvatochromic behavior with absorption maxima that range between 507 nm in MeOH and 590 nm in toluene (Table 6). This type of behavior has been observed with a number of $\text{Pt}(\text{diimine})(\text{dithiolate})$ complexes and has previously been assigned as a mixed metal/ligand-

Table 6. Charge-Transfer Absorption Maxima for Complexes **2a–2c** in Different Solvents^a

solvent	2a	2b	2c
pentane	574	586	585
toluene	578	590	589
Et ₂ O	572	583	582
CH ₂ Cl ₂	551	560	560
THF	567		578
DMSO	544	555	
MeCN	539	548	547
MeOH	496	508	507
	Solvatochromic Shift ^b		
2a	0.18		
2b	0.18		
2c	0.20		

^a 2.1×10^{-5} M in CH₂Cl₂:Solvent (1:4, v/v) at room temperature. $\lambda_{\text{abs}}/\text{nm}$.

^b Unitless slope from the plot of charge-transfer absorption maxima (eV) vs solvent parameter.²¹

to-ligand' charge-transfer (MMLL'CT) transition.^{19,21} Specifically, while the LUMO in these complexes is localized on a diimine π^* orbital, the HOMO has mixed Pt(d), S(p), and dithiolate ligand character. In the context of complexes **2a–2c**, a similar assignment involving a charge-transfer transition from an orbital of mixed metal-and-thiophenolate character to a π^* orbital localized on the C^{^N^N} ligand can be made. For the solvents examined in this study, the lower energy CT maxima, going from lowest energy to highest energy, are in the order toluene < pentane < Et₂O < THF < CH₂Cl₂ < DMSO < MeCN < MeOH. This order correlates well when comparing the energy of the CT band to the solvent polarity parameter value (Figure 5, inset) derived from the solvent dependent CT band in Pt(dbbpy)(tdt) (dbbpy = 4,4'-di-*tert*butyl-2,2'-bipyridine, tdt = toluene-3,4-dithiolate).^{21,23} The values for the solvatochromic shift for **2a**, **2b**, and **2c** are 0.18, 0.18, and 0.20, respectively, and are all lower in magnitude than those for reported Pt(diimine)(dithiolate)²¹ and Pt(diimine)bis(thiolate)²³ complexes, but are well within the range for a CT transition.^{21,23} The negative solvatochromism seen here and for the related Pt(diimine)(dithiolate) and bis(thiolate) complexes in which charge-transfer transition increases in energy with solvent polarity indicates that like those diimine systems, the Pt(C^{^N^N}) thiolate complexes possess a very polar ground state and a CT excited state in which the dipole is greatly diminished or even reversed.^{66–68}

(66) Huertas, S.; Hissler, M.; McGarrah, J. E.; Lachicotte, R. J.; Eisenberg, R. *Inorg. Chem.* **2001**, *40*, 1183–1188.

Conclusions

Three cyclometalated Pt(C^{^N^N}) thiophenolate complexes have been synthesized and characterized from newly designed 6-phenyl-2,2'-bipyridine ligands **L2** and **L3** and their Pt(C^{^N^N}) chloride precursors, **1a–1c**. Complexes **1a–1c** are luminescent in fluid CH₂Cl₂ solution with $\lambda_{\text{em}}^{\text{max}} \sim 575$ nm, assigned to a ³MLCT emissive state. The thiophenolate complexes **2a–2c** exhibit two charge-transfer bands in the electronic absorption spectrum tentatively assigned to a ¹CT ($\lambda_{\text{abs}} \sim 415$ nm) transition and a MMLL'CT ($\lambda_{\text{abs}} \sim 560$ nm in CH₂Cl₂) transition, respectively. The MMLL'CT band possesses interesting solvatochromic properties that are characteristic of a polar ground state and a charge-transfer excited state in which the dipole is greatly diminished. At room temperature and at 77 K, complexes **2a–2c** are not emissive and weakly emissive, respectively, when excited into the MMLL'CT absorption band in CH₂Cl₂ solution. However, **2a–2c** are emissive in CH₂Cl₂ solution when excited into the higher energy ¹CT band, with lifetimes between 135–305 ns ($\lambda_{\text{ex}} = 403$ nm), and the observed emission at ~ 550 nm is assigned to a charge-transfer to C^{^N^N} (³CT) emissive state, which we think has the same LUMO as suggested for **1a–1c** but possesses a different HOMO.

Acknowledgment. This work was supported by the Department of Energy, Division of Basic Sciences (DE-FG02-90ER14125). The authors also wish to acknowledge the following support from the University of Rochester: Elon Huntington Hooker Fellowship (P.D.), Graduate Assistance in Areas of National Need (GAANN) Fellowship (J.S.), and Weissberger Memorial Fellowship (J.S.). The authors also thank Prof. Todd Krauss for help in making possible the excited state lifetime measurements.

Supporting Information Available: Further details are given in Figures S1–S16; crystallographic data is given in CIF file format. This material is available free of charge via the Internet at <http://pubs.acs.org>.

IC801767Q

(67) Vanhelsmont, F. W. M.; Hupp, J. T. *Inorg. Chem.* **2000**, *39*, 1817–1819.

(68) Cummings, S. D.; Cheng, L.-T.; Eisenberg, R. *Chem. Mater.* **1997**, *9*, 440–450.